Radiated Susceptibility Test in Reverberation Chamber

MAGNUS HÖIJER

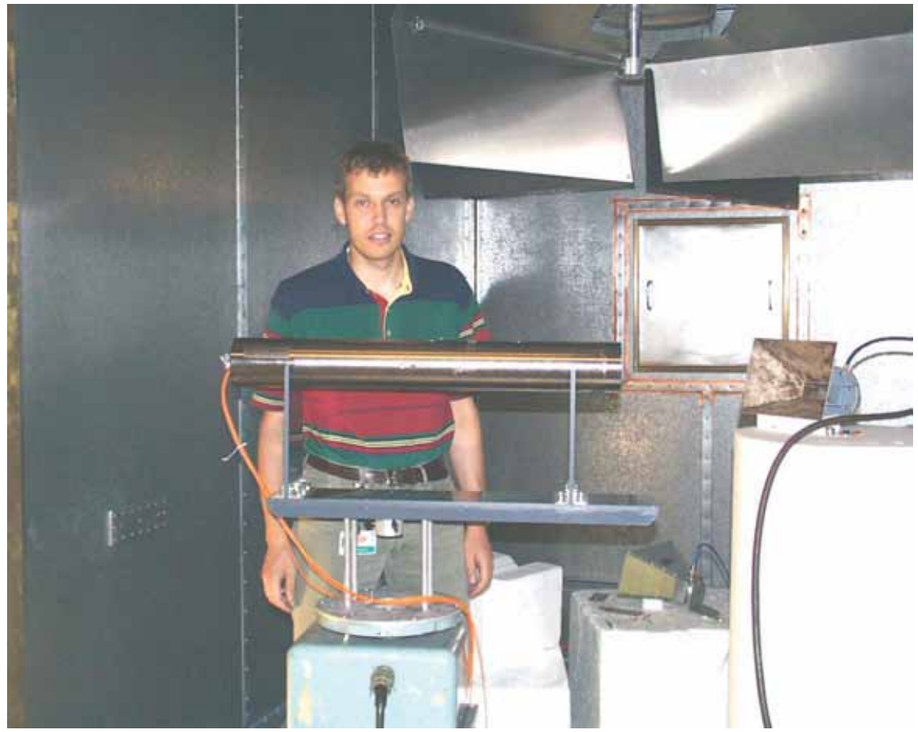

$$F_T(t) = \sum_{n=0}^{N} \binom{N}{n} (-1)^n \left(\frac{1}{1 + \frac{n}{N} t} \right)^N$$

FOI
Swedish Defence Research Agency
Sensor Technology
P.O. Box 1165
SE-581 11 Linköping

Phone: +46 13 37 80 00
Fax: +46 13 37 81 00

www.foi.se

FOI-R--2007--SE
ISSN 1650-1942

Scientific report
June 2006

Sensor Technology

Magnus Höijer

Radiated Susceptibility Test in Reverberation Chamber

FOI-R--2007--SE
ISSN 1650-1942

Scientific report
June 2006

Sensor Technology

Issuing organization	Report number, ISRN	Report type
FOI – Swedish Defence Research Agency Sensor Technology P.O. Box 1165 SE-581 11 Linköping	FOI-R--2007--SE	Scientific report
	Research area code 6. Electronic Warfare and deceptive measures	
	Month year June 2006	**Project no.** E 3031
	Sub area code 61 Electronic Warfare including Electromagnetic Weapons and Protection	
	Sub area code 2	

Author/s (editor/s)	Project manager
Dr. Magnus Höijer	Dr. Mats Bäckström
	Approved by Dr. Lena Klasén
	Sponsoring agency Swedish Armed Forces
	Scientifically and technically responsible Dr. Lars Pettersson

Report title
Radiated Susceptibility Test in Reverberation Chamber

Abstract

We show, by theory and experiment, that the stress put onto the equipment under test (EUT) when performing a radiated susceptibility test (RST) in a reverberation chamber (RC) is not affected by either the directivity pattern or the polarisation pattern of the EUT. The stress put onto the EUT will differ from the stress measured by a reference antenna in the RC. We have developed distribution functions for this discrepancy.

Keywords
Reverberation chamber (RC), radiated susceptibility test (RST), electromagnetic coupling, electromagnetic statistics, distribution functions

Further bibliographic information	Language English
ISSN 1650-1942	**Pages** 50 p.
	Price acc. to pricelist

Utgivare FOI - Totalförsvarets forskningsinstitut Sensorteknik Box 1165 581 11 Linköping	**Rapportnummer, ISRN** FOI-R--2007--SE	**Klassificering** Vetenskaplig rapport
	Forskningsområde 6. Telekrig och vilseledning	
	Månad, år Juni 2006	**Projektnummer** E 3031
	Delområde 61 Telekrigföring med EM-vapen och skydd	
	Delområde 2	
Författare/redaktör Dr. Magnus Höijer	**Projektledare** Dr. Mats Bäckström	
	Godkänd av Dr. Lena Klasén	
	Uppdragsgivare/kundbeteckning Försvarsmakten	
	Tekniskt och/eller vetenskapligt ansvarig Dr. Lars Pettersson	
Rapportens titel RS-test i modväxlande kammare		

Sammanfattning

Vi visar, teoretiskt såväl som experimentellt, att när en RS-testning utförs i en modväxlande kammare (MVK) så är den påkänning som vi utsätter vårt testobjekt för, oberoende av såväl testobjektets direktivitetsdiagram som dess polarisationsdiagram. Den påkänning som vi utsätter vårt testobjekt för skiljer sig från den påkänning som vi uppmäter i vår referensantenn. Vi har utvecklat fördelningsfunktioner för denna avvikelse.

Den praktiska betydelsen av detta resultat är att vi kan rekommendera att använda den modväxlande kammaren för RS-testning.

Nyckelord

Modväxlande kammare (MVK), RS-test (RST), elektromagnetisk koppling, elektromagnetisk statistik, fördelningsfunktioner

Övriga bibliografiska uppgifter	**Språk** Engelska
ISSN 1650-1942	**Antal sidor:** 50 s.
Distribution enligt missiv	**Pris: Enligt prislista**

Contents

1 Introduction **1**

2 Theory **3**
2.1 Electromagnetic Field in the Reverberation Chamber 3
2.2 Received Power in the Critical Component of the Equipment Under Test 7
2.3 The Maximum Received Power in the Critical Component of the Equipment Under Test 12
2.3.1 Z-distribution 12
2.3.2 T-distribution 14
2.3.3 A-distribution 16

3 Experiments **23**
3.1 Antennas as Equipment Under Test 23
3.2 Real Test Objects as Equipment Under Test 25
3.3 Experiments on the A-distribution 27

4 Practical Advice on using the Reverberation Chamber for Radiated Susceptibility Testing **29**
4.1 Using Maximum Values 30
4.2 Using Average Values 33
4.3 Comparing the Average Value Method to the Maximum Value Method 34

5 Summary **39**

Acknowledgement **40**

A An Integral **41**

References **43**

Chapter 1

Introduction

Most of the work performed by the Reverberation Chamber (RC) community has been focused on characterising the RC. Important contributions to the understanding of the electromagnetic environment in the RC has been given by many within the community including Kostas and Boverie [1], Hill [2], [3] and Lehman [4]. Characterising the chamber is an essential property in quantifying the magnitude of the stress we put onto our Equipment Under Test (EUT) during a Radiated Susceptibility Test (RST).

The outcome of a Radiated Susceptibility Test (RST) does however also depend on how efficiently the electromagnetic field couples to the most fragile components in the Equipment Under Test (EUT). Hill [2], [3] does here provide important theoretical understanding. Hill derives, outgoing from a plane wave description, an expression for the power absorbed by an antenna placed in the RC, and makes the important statement that an EUT is nothing but a lossy impedance-mismatched antenna. The most critical components in the EUT can be seen as nothing else than loads to the antennas which the EUT constitutes.

When the RST is performed at an Open Area Test Site (OATS) or in an Anechoic Chamber (AC) the result is strongly affected by from which direction the EUT is irradiated as well as the polarisation in use. That can physically be described by the directivity and the receiving polarisation of the EUT, as well as the polarisation of the electromagnetic field incident on the EUT. The quantitative importance of the directivity and the receiving polarisation of the EUT, has experimentally been shown by Coupling Measurements (CM) [5], [6], but also by true high level Radiated Susceptibility Testing (RST) [5], [7].

A relevant question is if the directivity and receiving polarisation of the EUT will affect the result of an RST in the RC, and/or are there any other similar parameters affecting the outcome of an RST in an RC? It seems to be generally accepted within the community that the directivity of the EUT does not affect the outcome of an RST in the RC. Some say that "the RC washes out the directivity". The expression is strictly speaking wrong because the directivity is only a property of the EUT, and it remains unaffected by that the EUT is placed inside the RC. Anyhow the expression is a simple way to state that if an RST is performed with two EUT's whose directivity

patterns differ, but all other antenna parameters equal, the outcome of the RST is the same for the two EUT's. Though very seldom pointed out, the receiving polarisation of the EUT does also not affect the result of an RST in the RC, so a similar simple expression could be that the "the RC washes out the directivity and the receiving polarisation".

A theoretical description of why the directivity does not affect the outcome of an RST in the RC, is again given by Hill [2], [3]. Hill derives an expression for the power received by an antenna.[1] He shows that the ensemble average of the power received by the antenna taken over many independent stirrer positions is independent of the directivity of the EUT. But Hill does not stop there, he goes further, he derives a probability density function for the power received by an antenna in the RC. That is good, because it gives us an opportunity to address the important question, what is the maximum stress we impose onto the critical component in the EUT when performing an RST in the RC? We are actually often not so interested in the average stress (taken over many independent stirrer positions) which we impose onto the EUT, but more interested in the maximum stress imposed onto the EUT.

We assumed that the directivity of the EUT would be a parameter affecting the maximum stress we put onto the critical component in the EUT. One might assume that for an EUT with a large maximum directivity, the electromagnetic field inside the RC and the most susceptible direction of the EUT would for one of the stirrer positions "co-operate" so that the electromagnetic energy couples more efficiently to the most critical component in the EUT, than it would for an EUT with a small maximum directivity. If that is true, an EUT with a larger maximum directivity *would* be more susceptible, just as a corresponding accurate RST at an OATS or in an AC shows. However, by examining and manipulating the expressions by Hill [2], [3], we find the opposite: The directivity of the EUT does not affect the outcome of an RST in the RC, and that despite that we are interested in the maximum electromagnetic energy which couples to the critical component in the EUT, where the maximum is taken over many independent stirrer positions.

The purpose of this report is to put some light onto that contradictory issue. We will also show experimental results, and give some practical advice on how to use the Reverberation Chamber for Radiated Susceptibility Testing.

[1] The reader should think that "received by antenna" equals "received by the most critical component in the EUT".

Chapter 2

Theory

In this chapter we will derive distribution functions for the received power in the Equipment Under Test (EUT). In doing so we will to a large extent benefit from the plane wave model proposed by Hill [2], [3]. However, we will by generalising some of assumptions proposed by Hill show that no other distribution functions may describe the electromagnetic field in the Reverberation Chamber (RC) as well as the power received by the EUT. We assume, or rather state, that an EUT is nothing but a set of lossy impedance-mismatched antennas. Power will be absorbed in many parts of the EUT, but we are only interested in the power delivered to the very most critical component in the EUT. The rest of the power being absorbed in the EUT is most often the bulk of the power being absorbed in the EUT, and a part of it constitutes the losses in our antenna model.

We will derive statistical expressions for the current delivered to the critical component in the EUT. Knowing the resistance of the critical component it is easy to calculate the power absorbed in it. Outgoing from these expression for the power absorbed in the critical component of the EUT, we will see that the maximum value statistics for the RC given in [8] and [9] is applicable here as well.

We will assume time harmonic fields and use a phasor notation for the fields. E.g. the phasor notation for the electric field is $\boldsymbol{E}(\boldsymbol{r},\omega)$, and the real electric field is,

$$\boldsymbol{E}(\boldsymbol{r},t) = \mathrm{Re}\left\{\boldsymbol{E}(\boldsymbol{r},\omega)e^{-i\omega t}\right\} \ . \tag{2.1}$$

We will most often not explicitly include the frequency dependence in our notations.

2.1 Electromagnetic Field in the Reverberation Chamber

We start by describing the electromagnetic environment of the Reverberation Chamber. The field distribution inside the chamber is complex, but the electric field ($\boldsymbol{E}$) inside a spherical source-free region can always be described as a sum of plane waves over all real solid angles (Ω) [10], [11],

$$\boldsymbol{E}(\boldsymbol{r}) = \iint_{4\pi} \boldsymbol{F}(\hat{\boldsymbol{k}}) e^{ik\hat{\boldsymbol{k}}\cdot\boldsymbol{r}} \mathrm{d}\Omega \ , \tag{2.2}$$

where $\boldsymbol{F}$ is the solid angle spectrum of the electric field, k is the wave number and $\hat{\boldsymbol{k}}$ is the unit vector of the wave vector ($\boldsymbol{k} = k\hat{\boldsymbol{k}}$) of the plane wave within the infinitesimal solid angle $\mathrm{d}\Omega$. The direction of $\hat{\boldsymbol{k}}$ is completely defined by the two spherical coordinates α and β,[1]

$$\hat{\boldsymbol{k}}(\alpha, \beta) = (\sin\alpha\cos\beta\hat{\boldsymbol{x}} + \sin\alpha\sin\beta\hat{\boldsymbol{y}} + \cos\alpha\hat{\boldsymbol{z}}) \ . \tag{2.3}$$

Equation (2.2) is valid within a source free region, and introducing an EUT into that region makes the condition no longer fulfilled for the total field in that region. However, and this is important, we are not interested in the total field in the Reverberation Chamber (RC), but the field incident on the EUT. It is only the incident field on the EUT which stresses the component inside the EUT. The EUT is not directly affected by the, from the EUT, scattered field.[2] For the incident field we can superpose away the EUT and do a continuation of the field through the whole spherical region. Hence, (2.2) is valid for the interesting incident field. Often one introduce a subindex i to denote that the field is the incident field. We will avoid doing that, because we think we can increase the readability of this article by limiting the number of indices. However, it is to be remembered that the fields we treat, are the fields incident on the EUT, and not the total fields.

Just like Hill [2], [3], we decompose the solid angle spectrum into two orthogonal components in the α and β directions,

$$\boldsymbol{F}(\hat{\boldsymbol{k}}) = \left[F_{\alpha r}(\hat{\boldsymbol{k}}) + iF_{\alpha i}(\hat{\boldsymbol{k}})\right]\hat{\boldsymbol{\alpha}} + \left[F_{\beta r}(\hat{\boldsymbol{k}}) + iF_{\beta i}(\hat{\boldsymbol{k}})\right]\hat{\boldsymbol{\beta}} \ , \tag{2.4}$$

where we explicitly have written the components in terms of their real and imaginary parts. The four real components in (2.4) ($F_{\alpha r}, F_{\alpha i}, F_{\beta r}, F_{\beta i}$) does (for every direction $\hat{\boldsymbol{k}}$) completely describe the solid angle spectrum $\boldsymbol{F}(\hat{\boldsymbol{k}})$.

We now start a statistical approach to describe the complex electromagnetic field in the Reverberation Chamber. We assume that all four real components ($F_{\alpha r}, F_{\alpha i}, F_{\beta r}, F_{\beta i}$) are random variables, that they have the same distributions functions, that they are completely uncorrelated among themselves and that there is no

[1] It is the well-established practice to let the letters θ and ϕ denote the spherical coordinates. However, we will here us the practice to let the letters θ and ϕ denote the spherical coordinates of the radius vector and let α and β denote the spherical coordinates of the wave vector [10, p. 361-362].

[2] Indirectly the EUT is affected by the scattered field because the field is rescattered at walls, stirrers, antennas and other possible objects placed in the RC. However we assume that all this rescattered field will not make the assumptions, which we will make for the field incident on the EUT, less valid. Actually in opposite, we think that the EUT itself is essential in providing the complex field environment which we assume for the RC. That assumption is to be further investigated.

preferable phase. We also assume that the same component for two different directions are uncorrelated. Those assumptions imply the following expected values for the four real components,

$$\mathbb{E}\left\{F_{AB}(\hat{\boldsymbol{k}})\right\} = 0 \tag{2.5}$$

and

$$\mathbb{E}\left\{F_{A_1B_1}(\hat{\boldsymbol{k}}_1)F_{A_2B_2}(\hat{\boldsymbol{k}}_2)\right\} = C^2\delta_{A_1A_2}\delta_{B_1B_2}\delta(\hat{\boldsymbol{k}}_1 - \hat{\boldsymbol{k}}_2) \ , \tag{2.6}$$

where the variables $\hat{\boldsymbol{k}}_1$ and $\hat{\boldsymbol{k}}_2$ are two samples from the set of all directions of the wave vector ($\{\hat{\boldsymbol{k}}\}$),

$$\hat{\boldsymbol{k}}_1, \hat{\boldsymbol{k}}_2 \in \{\hat{\boldsymbol{k}}\} \ , \tag{2.7}$$

the index A is one of the two spherical coordinates α and β,

$$A \in \{\alpha, \beta\} \ , \tag{2.8}$$

and the index B denotes the real (r) or imaginary (i) part,

$$B \in \{r, i\} \ . \tag{2.9}$$

The subindices 1 and 2 in (2.6) are introduced to allow for the possibility of different indices of the two quantities in (2.6). On the right hand side of (2.6), C is a constant,[3] the two first deltas are Kronecker deltas,[4] and the last delta is the Dirac delta pulse.[5]

The equations in (2.5) and (2.6) are not new. They are actually nothing but equations (5)-(7) in [2], or (31)-(33) in [3], written in a compact form.[6] Now we will go a step further by generalising the assumptions in (2.5) and (2.6). Equation (2.5) and (2.6) are the first and second order moments [13, p. 31] of the random variable $F_{AB}(\hat{\boldsymbol{k}})$. We do the following rather natural assumptions for the third and forth order moments,

---

[3]The square of the constant is proportional to the energy density in the RC. We will not calculate the constant here, see [2] and [3] for a further description.

[4]The Kronecker delta:

$$\delta_{A_mA_n} = \begin{cases} 1, & A_m = A_n \\ 0, & A_m \neq A_n \end{cases} \tag{2.10}$$

[5]The Dirac delta pulse ($\boldsymbol{f}(\hat{\boldsymbol{k}})$ is a general vector field):

$$\iint\limits_{4\pi} \boldsymbol{f}(\hat{\boldsymbol{k}}_1)\delta(\hat{\boldsymbol{k}}_1 - \hat{\boldsymbol{k}}_2)\mathrm{d}\Omega_1 = \boldsymbol{f}(\hat{\boldsymbol{k}}_2) \tag{2.11}$$

[6]To be correct there is a difference; In [2] and [3] the notation <> represents the ensemble average over many independent stirrer positions, but here the notation $\mathbb{E}\{\}$ represents the expected value. When performing a measurement in the RC of the expected value, we do measure the ensemble average over many independent stirrer positions. The approximation we thereby introduce is not negligible, as can be seen in [12].

$$\mathbb{E}\left\{F_{A_1B_1}(\hat{\boldsymbol{k}}_1)F_{A_2B_2}(\hat{\boldsymbol{k}}_2)F_{A_3B_3}(\hat{\boldsymbol{k}}_3)\right\} = 0 \ , \tag{2.12}$$

and

$$\begin{aligned}
&\mathbb{E}\left\{F_{A_1B_1}(\hat{\boldsymbol{k}}_1)F_{A_2B_2}(\hat{\boldsymbol{k}}_2)F_{A_3B_3}(\hat{\boldsymbol{k}}_3)F_{A_4B_4}(\hat{\boldsymbol{k}}_4)\right\} \\
&\quad = C^4\delta_{A_1A_2}\delta_{B_1B_2}\delta(\hat{\boldsymbol{k}}_1-\hat{\boldsymbol{k}}_2)\delta_{A_3A_4}\delta_{B_3B_4}\delta(\hat{\boldsymbol{k}}_3-\hat{\boldsymbol{k}}_4) \\
&\quad +C^4\delta_{A_1A_3}\delta_{B_1B_3}\delta(\hat{\boldsymbol{k}}_1-\hat{\boldsymbol{k}}_3)\delta_{A_2A_4}\delta_{B_2B_4}\delta(\hat{\boldsymbol{k}}_2-\hat{\boldsymbol{k}}_4) \\
&\quad +C^4\delta_{A_1A_4}\delta_{B_1B_4}\delta(\hat{\boldsymbol{k}}_1-\hat{\boldsymbol{k}}_4)\delta_{A_2A_3}\delta_{B_2B_3}\delta(\hat{\boldsymbol{k}}_2-\hat{\boldsymbol{k}}_3) \\
&\quad = C^4 \underset{l,m\leq 4}{\Delta} \delta_{A_lA_m}\delta_{B_lB_m}\delta(\hat{\boldsymbol{k}}_l-\hat{\boldsymbol{k}}_m) \ ,
\end{aligned} \tag{2.13}$$

where we in the last step have introduced a shorthand notation by introducing the Δ-operator. The Δ-operator includes both multiplications and additions and can be understood by looking on (2.13). First we take the product of 2 Kronecker deltas times 2 Kronecker deltas times 2 Dirac delta pulses. The indices are placed two and two on the Kronecker deltas and are increased consecutively from A_1 to A_4 on the first 2 Kronecker deltas and from B_1 to B_4 on the last 2 Kronecker deltas. The indices also comes two and two in the delta pulses and are also increased consecutively from 1 to 4. That's the first product (and first row after the equal sign) in (2.13). The Δ-operator does also include adding to the first product, all products which are permutations of the integers in the first product and do not equal the first product.[7] In total there are $(4-1)!! = 3\cdot 1 = 3$ products to be summed.[8]

The good thing with introducing the Δ-operator is that we now can write an expression for a natural assumption for the n:th moment of the random variable $F_{AB}(\hat{\boldsymbol{k}})$,

$$\mathbb{E}\left\{\prod_{j=1}^{n} F_{A_jB_j}(\hat{\boldsymbol{k}}_j)\right\} = \begin{cases} C^n \underset{l,m\leq n}{\Delta} \delta_{A_lA_m}\delta_{B_lB_m}\delta(\hat{\boldsymbol{k}}_l-\hat{\boldsymbol{k}}_m), & n \text{ even} \\ 0, & n \text{ odd} \end{cases} \tag{2.15}$$

where the n:th order Δ-operation is to be understood as follows: First take the product of $n/2$ Kronecker deltas times $n/2$ Kronecker deltas times $n/2$ Dirac delta pulses. The indices are placed two and two on the Kronecker deltas and are increased consecutively from A_1 to A_n on the first $n/2$ Kronecker deltas and from B_1 to B_n on the last $n/2$ Kronecker deltas. The indices also comes two and two in the delta pulses

[7] Hence, the permutations of the indices within the Kronecker deltas and the delta pulses are not to be included because $\delta_{A_lA_m} \equiv \delta_{A_mA_l}$ and $\delta(\hat{\boldsymbol{k}}_l-\hat{\boldsymbol{k}}_m) \equiv \delta(\hat{\boldsymbol{k}}_m-\hat{\boldsymbol{k}}_l)$.

[8] Semi-factorial for the positive integer n is defined as:

$$n!! = \begin{cases} n\cdot n-2\cdot ...\cdot 4\cdot 2, & n \text{ even} \\ n\cdot n-2\cdot ...\cdot 3\cdot 1, & n \text{ odd} \end{cases} \tag{2.14}$$

and are also increased consecutively from 1 to n. That's the first product. Calculate all products which are permutations of the integers in the first product and do not equal the first product. The final results is found by summing up all these $(n-1)!!$ products.

Equation (2.15) may look very complicated, but might be understood as simply a generalisation of (2.5),(2.6),(2.12) and (2.13). The good thing is that (2.15) is the only assumption we have to do about the field in the RC.

2.2 Received Power in the Critical Component of the Equipment Under Test

We will now try to find an expression for the distribution function of the power absorbed in the critical component of the EUT. To do that we will start with an expression of the current which flows through the critical component of the EUT. From the Critical component, the EUT is seen as an antenna, and for every direction $(\hat{\boldsymbol{r}})$, the antenna has the complex receiving function,

$$\boldsymbol{Y}(\hat{\boldsymbol{r}}) = [Y_{\theta r}(\hat{\boldsymbol{r}}) + iY_{\theta i}(\hat{\boldsymbol{r}})]\,\hat{\boldsymbol{\theta}} + [Y_{\varphi r}(\hat{\boldsymbol{r}}) + iY_{\varphi i}(\hat{\boldsymbol{r}})]\,\hat{\boldsymbol{\varphi}}\ , \tag{2.16}$$

defined in such a way that the total current which flows through the critical component of the EUT is,

$$\begin{aligned} I &= \iint\limits_{4\pi}\iint\limits_{4\pi} \boldsymbol{Y}(\hat{\boldsymbol{r}})\cdot\boldsymbol{F}(\hat{\boldsymbol{k}})\delta(\hat{\boldsymbol{r}}+\hat{\boldsymbol{k}})\mathrm{d}\Omega_{\hat{\boldsymbol{r}}}\mathrm{d}\Omega_{\hat{\boldsymbol{k}}} \\ &= \iint\limits_{4\pi} \boldsymbol{Y}(\hat{\boldsymbol{r}})\cdot\boldsymbol{F}(-\hat{\boldsymbol{r}})\mathrm{d}\Omega\ . \end{aligned} \tag{2.17}$$

By plugging (2.4) and (2.16) into (2.17) we get,

$$I = I_r + iI_i\ , \tag{2.18}$$

where the quadrature components of the current are,[9]

$$\begin{aligned} I_r &= \iint\limits_{4\pi} [Y_{\theta r}(\hat{\boldsymbol{r}})F_{\alpha r}(-\hat{\boldsymbol{r}}) - Y_{\theta i}(\hat{\boldsymbol{r}})F_{\alpha i}(-\hat{\boldsymbol{r}}) \\ &- Y_{\varphi r}(\hat{\boldsymbol{r}})F_{\beta r}(-\hat{\boldsymbol{r}}) + Y_{\varphi i}(\hat{\boldsymbol{r}})F_{\beta i}(-\hat{\boldsymbol{r}})]\,\mathrm{d}\Omega\ , \end{aligned} \tag{2.19}$$

and

[9]Note that $\hat{\boldsymbol{\alpha}}(-\hat{\boldsymbol{r}}) = \hat{\theta}(\hat{\boldsymbol{r}})$, but $\hat{\boldsymbol{\beta}}(-\hat{\boldsymbol{r}}) = -\hat{\boldsymbol{\varphi}}(\hat{\boldsymbol{r}})$.

$$
\begin{aligned}
I_i &= \iint\limits_{4\pi} \left[Y_{\theta r}(\hat{\boldsymbol{r}}) F_{\alpha i}(-\hat{\boldsymbol{r}}) + Y_{\theta i}(\hat{\boldsymbol{r}}) F_{\alpha r}(-\hat{\boldsymbol{r}}) \right. \\
&- \left. Y_{\varphi r}(\hat{\boldsymbol{r}}) F_{\beta i}(-\hat{\boldsymbol{r}}) - Y_{\varphi i}(\hat{\boldsymbol{r}}) F_{\beta r}(-\hat{\boldsymbol{r}}) \right] \mathrm{d}\Omega \ . \qquad (2.20)
\end{aligned}
$$

With help of (2.5) we find that,

$$
\mathbb{E}\left\{ I_r \right\} = \mathbb{E}\left\{ I_i \right\} = 0 \ , \qquad (2.21)
$$

and with help of (2.6) we find that,

$$
\begin{aligned}
\mathbb{E}\left\{ I_r^2 \right\} &= \iint\limits_{4\pi} \iint\limits_{4\pi} \mathbb{E}\Big\{ \left[Y_{\theta r}(\hat{\boldsymbol{r}}_1) F_{\alpha r}(-\hat{\boldsymbol{r}}_1) + Y_{\theta i}(\hat{\boldsymbol{r}}_1) F_{\alpha i}(-\hat{\boldsymbol{r}}_1) \right. \\
&- \left. Y_{\varphi r}(\hat{\boldsymbol{r}}_1) F_{\beta r}(-\hat{\boldsymbol{r}}_1) - Y_{\varphi i}(\hat{\boldsymbol{r}}_1) F_{\beta i}(-\hat{\boldsymbol{r}}_1) \right] \\
&\times \left[Y_{\theta r}(\hat{\boldsymbol{r}}_2) F_{\alpha r}(-\hat{\boldsymbol{r}}_2) + Y_{\theta i}(\hat{\boldsymbol{r}}_2) F_{\alpha i}(-\hat{\boldsymbol{r}}_2) \right. \\
&- \left. Y_{\varphi r}(\hat{\boldsymbol{r}}_2) F_{\beta r}(-\hat{\boldsymbol{r}}_2) - Y_{\varphi i}(\hat{\boldsymbol{r}}_2) F_{\beta i}(-\hat{\boldsymbol{r}}_2) \right] \Big\} \mathrm{d}\Omega_1 \mathrm{d}\Omega_2 \\
&= C^2 \iint\limits_{4\pi} \left[Y_{\theta r}^2(\hat{\boldsymbol{r}}) + Y_{\theta i}^2(\hat{\boldsymbol{r}}) + Y_{\varphi r}^2(\hat{\boldsymbol{r}}) + Y_{\varphi i}^2(\hat{\boldsymbol{r}}) \right] \mathrm{d}\Omega \\
&= C^2 \iint\limits_{4\pi} \left[\left| Y_\theta(\hat{\boldsymbol{r}}) \right|^2 + \left| Y_\varphi(\hat{\boldsymbol{r}}) \right|^2 \right] \mathrm{d}\Omega \ . \qquad (2.22)
\end{aligned}
$$

We can already here see one interesting property, the integral in (2.22) is only a function of the properties of the EUT, and hence the influence on the result from the RC is only through the constant C.

The integral in (2.22) can be rewritten in more common antenna quantities. The power received in an antenna from a plane wave, with the electric field vector $\boldsymbol{E} = E\hat{\boldsymbol{e}}$, incident on the antenna is [14, pp. 86], [15, pp. 64],

$$
P = q\eta p(\hat{\boldsymbol{r}}, \hat{\boldsymbol{e}}) D(\hat{\boldsymbol{r}}) \frac{\lambda^2}{4\pi} \frac{E^2}{2Z_0} \ , \qquad (2.23)
$$

where q is the impedance mismatch factor, η the radiation efficiency and D the directivity of the antenna. The factor p is the polarisation efficiency between the antenna and the incident field, λ and $\boldsymbol{E}_0$ are the wavelength and electric field vector, respectively, of the incident electromagnetic field and $Z_0 (\approx 377\Omega)$ is the wave impedance of free space. Looking upon how the complex receiving function ($Y(\hat{\boldsymbol{r}})$) and the solid angle spectrum of the electric field ($F(\hat{\boldsymbol{k}})$) is defined through (2.2), (2.16) and (2.17), the power (P) does also equal,

$$
P = \frac{R\left|I\right|^2}{2} = \frac{R\left|\boldsymbol{Y}(\hat{\boldsymbol{r}}) \cdot \boldsymbol{E}\right|^2}{2} = Rp(\hat{\boldsymbol{r}}, \hat{\boldsymbol{e}}) \left[\left| Y_\theta(\hat{\boldsymbol{r}}) \right|^2 + \left| Y_\varphi(\hat{\boldsymbol{r}}) \right|^2 \right] \frac{E^2}{2} \ , \qquad (2.24)
$$

where R is the resistance of the load to the antenna, or in our case, the resistance of the most critical component in the EUT. The last step in (2.24) follows directly from the definition of the polarisation efficiency [14, p. 70], [15, p. 66]. With help of (2.23) and (2.24), and that it follows directly from the definition of the directivity [16] that the average directivity,

$$\frac{1}{4\pi}\iint\limits_{4\pi} D(\hat{\boldsymbol{r}})\mathrm{d}\Omega = 1 \ , \tag{2.25}$$

we can conclude that,

$$\iint\limits_{4\pi} \left[|Y_\theta(\hat{\boldsymbol{r}})|^2 + |Y_\varphi(\hat{\boldsymbol{r}})|^2\right] \mathrm{d}\Omega = \frac{\eta q \lambda^2}{RZ_0} \ , \tag{2.26}$$

and with (2.26) plugged into (2.22),

$$\mathbb{E}\left\{I_r^2\right\} = C^2\frac{\eta q \lambda^2}{RZ_0} \ . \tag{2.27}$$

In complete similarity it can be shown that the variance of the imaginary part of the current ($\mathbb{E}\left\{I_i^2\right\}$) has the same value,

$$\mathbb{E}\left\{I_i^2\right\} = \mathbb{E}\left\{I_r^2\right\} = C^2\frac{\eta q \lambda^2}{RZ_0} \ , \tag{2.28}$$

and it is therefore natural to introduce the notation,[10]

$$\sigma \triangleq \sqrt{\mathbb{E}\left\{I_i^2\right\}} = \sqrt{\mathbb{E}\left\{I_r^2\right\}} = C\sqrt{\frac{\eta q}{RZ_0}}\lambda \ , \tag{2.29}$$

for the standard deviation of the two quadrature components of the current in the critical component of the EUT.

We have in (2.21) and (2.28) expressions for the first and second order moments of the two quadrature components of the current. We will now turn to higher order moments. With help of (2.4), (2.12), (2.16), (2.17) and (2.18), we find that,

$$\begin{aligned}
\mathbb{E}\left\{I_r^3\right\} &= \iint\limits_{4\pi}\iint\limits_{4\pi}\iint\limits_{4\pi} \mathbb{E}\Big\{\mathrm{Re}\left\{\boldsymbol{Y}(\hat{\boldsymbol{r}}_1)\cdot\boldsymbol{F}(-\hat{\boldsymbol{r}}_1)\right\} \\
&\times \mathrm{Re}\left\{\boldsymbol{Y}(\hat{\boldsymbol{r}}_2)\cdot\boldsymbol{F}(-\hat{\boldsymbol{r}}_2)\right\} \times \mathrm{Re}\left\{\boldsymbol{Y}(\hat{\boldsymbol{r}}_3)\cdot\boldsymbol{F}(-\hat{\boldsymbol{r}}_3)\right\}\Big\}\mathrm{d}\Omega_1\mathrm{d}\Omega_2\mathrm{d}\Omega_3 \\
&= 0 \ ,
\end{aligned} \tag{2.30}$$

and with (2.4), (2.13), (2.16), (2.17), (2.18), (2.26), (2.29) and by studying the principles in (2.22) we find after some arithmetics that,

[10] The sign $\triangleq$ denote *defined as*.

$$\begin{aligned}\mathbb{E}\left\{I_r^4\right\} &= \iint_{4\pi}\iint_{4\pi}\iint_{4\pi}\mathbb{E}\Big\{\mathrm{Re}\left\{\boldsymbol{Y}(\hat{\boldsymbol{r}}_1)\cdot\boldsymbol{F}(-\hat{\boldsymbol{r}}_1)\right\}\times\mathrm{Re}\left\{\boldsymbol{Y}(\hat{\boldsymbol{r}}_2)\cdot\boldsymbol{F}(-\hat{\boldsymbol{r}}_2)\right\}\\ &\times\ \mathrm{Re}\left\{\boldsymbol{Y}(\hat{\boldsymbol{r}}_3)\cdot\boldsymbol{F}(-\hat{\boldsymbol{r}}_3)\right\}\times\mathrm{Re}\left\{\boldsymbol{Y}(\hat{\boldsymbol{r}}_4)\cdot\boldsymbol{F}(-\hat{\boldsymbol{r}}_4)\right\}\Big\}\mathrm{d}\Omega_1\mathrm{d}\Omega_2\mathrm{d}\Omega_3\mathrm{d}\Omega_4\\ &= \sigma^4(4-1)!! = 3\sigma^4\ . \end{aligned} \tag{2.31}$$

It can also be shown that,

$$\mathbb{E}\left\{I_i^3\right\} = \mathbb{E}\left\{I_r^3\right\} = 0\ , \tag{2.32}$$

and

$$\mathbb{E}\left\{I_i^4\right\} = \mathbb{E}\left\{I_r^4\right\} = 3\sigma^4\ . \tag{2.33}$$

The general n:th moment of the quadrature components of the current in the critical component of the EUT is with the assumptions in (2.15) found to be,

$$\mathbb{E}\left\{I_i^n\right\} = \mathbb{E}\left\{I_r^n\right\} = \frac{(1+(-1)^n)}{2}(n-1)!!\ \sigma^n\ . \tag{2.34}$$

Hence, outgoing only from the assumptions in (2.15) about the field in the Reverberation Chamber, we have managed to calculate all moments for the distribution of the quadrature components of the current. We can also calculate the moment generating function [13, p. 100],

$$\begin{aligned}M(s) &= \sum_{n=0}^{\infty}\frac{\mathbb{E}\left\{I_r^n\right\}}{n!}s^n = \sum_{n=0}^{\infty}\frac{(2n-1)!!}{(2n)!}\sigma^{2n}s^{2n} = \sum_{n=0}^{\infty}\frac{(2n-1)!!2^n}{(2n)!}\left(\frac{\sigma s}{2}\right)^{2n}\\ &= \left\{(r-1)!! = \frac{r!}{2^{\frac{r}{2}}(r/2)!}\right\} = \sum_{n=0}^{\infty}\frac{1}{n!}\left(\frac{\sigma^2s^2}{2}\right)^n = e^{\frac{\sigma^2s^2}{2}}\ . \end{aligned} \tag{2.35}$$

The theory of analytic continuation of functions justifies to do the substitution $s = it$ [11] [13, p. 104], and we get the characteristic function [13, p. 100],

$$\phi(t) = M(it) = e^{-\frac{\sigma^2t^2}{2}}\ . \tag{2.36}$$

Knowing the characteristic function of a distribution function is very good, because the probability density function is nothing but the Fourier transform of the characteristic function [13, p. 106], and hence the probability density functions for the quadrature components of the current are found to be,[12]

[11] $i = \sqrt{-1}$

[12] The element i_r (i_i) is an element in the domain of the probability density function of the random variable I_r (I_i).

$$\begin{aligned} f_{I_r}(i_r) &= \frac{1}{2\pi}\int_{-\infty}^{\infty} e^{-ii_r t}\phi(t)\mathrm{d}t = \frac{1}{2\pi}\mathfrak{F}\left\{\phi(t)\right\} = \frac{1}{2\pi}\mathfrak{F}\left\{e^{-\frac{\sigma^2 t^2}{2}}\right\} = \frac{1}{2\pi}\frac{\sqrt{2\pi}}{\sigma}e^{-\frac{i_r^2}{2\sigma^2}} \\ &= \frac{1}{\sqrt{2\pi}\sigma}e^{-\frac{i_r^2}{2\sigma^2}} \ , \end{aligned} \tag{2.37}$$

and,

$$f_{I_i}(i_i) = \frac{1}{\sqrt{2\pi}\sigma}e^{-\frac{i_i^2}{2\sigma^2}} \ , \tag{2.38}$$

which is the probability density function of the normal (Gaussian) distribution. We conclude that the quadrature components of the current in the critical component of the EUT are normally distributed with expected value 0 and standard deviation σ,

$$I_i, I_r \in N[0, \sigma] \ . \tag{2.39}$$

We have already assumed that the resistance of the critical component in the EUT is R, so the critical component absorbs the power,

$$P = \frac{R\left|I\right|^2}{2} = \frac{R(I_r^2 + I_i^2)}{2} \ , \tag{2.40}$$

and outgoing from the underlying distribution functions (2.37) and (2.38) it can be shown [17, p. 227] that the power absorbed in the critical component is exponentially distributed,

$$f_P(p) = \frac{1}{R\sigma^2}e^{-\frac{p}{R\sigma^2}} \equiv \frac{1}{\mathbb{E}\left\{P\right\}}e^{-\frac{p}{\mathbb{E}\{P\}}} \ , \tag{2.41}$$

where we in the last step have introduced that the expected value (as well as the standard deviation) of the exponential distribution in (2.41) is,

$$\mathbb{E}\left\{P\right\} = R\sigma^2 = C^2\frac{\eta q \lambda^2}{Z_0} \ . \tag{2.42}$$

To derive and propose (2.41) as the distribution function for the power absorbed in the critical component of the EUT was the objective of this section and actually (2.41) is the same equation as the forth equation in [1] and (66) in [2] or (90) in [3]. However, as very well pointed out by Hill in [2, p. 215] and [3, p. 21], the derivation here as well as in [2] and [3] is more general because it is a derivation of the power being absorbed in the critical component of the EUT. The proposed forth equation in [1] is actually only a distribution function for the square of the absolute value of the electric field in one arbitrary direction. Further on, the theory presented here is more definitive than the theory in [2] and [3], because the derivation in [2] and [3], which is based on maximising the entropy, leaves open for that some additional information would

change the distribution function [3, p. 18]. Here, (2.15) is a sufficient assumption about the field in the RC to be able to describe the power received by the critical component in the EUT. Any additional assumption about the field in the RC, will

1. Already be included in (2.15), or
2. Contradict (2.15).

2.3 The Maximum Received Power in the Critical Component of the Equipment Under Test

2.3.1 Z-distribution

In performing a Radiated Susceptibility Test (RST) in the Reverberation Chamber (RC), the Equipment Under Test (EUT) is stressed for N different stirrer positions.[13] The number of N may typically be in the range from a few tens to a few hundred. By presupposing that the power absorbed by the critical component for every stirrer position is independent of all the other $N-1$ stirrer positions [9], [18], we get N random samples from the distribution function in (2.41). In performing an RST, the interesting parameter is the maximum value taken over all N stirrer positions. Also the maximum value is a random variable, and it can easily be calculated from (2.41). Before doing so we will however first introduce the quantity normalised power,

$$X \triangleq \frac{P}{\mathbb{E}\{P\}} , \tag{2.43}$$

as the power received in the critical component divided by the expected value of that power. It follows from (2.41) that the normalised power has the probability distribution function,

$$f_X(x) = e^{-x} , \tag{2.44}$$

and the cumulative distribution function is,

$$F_X(x) = 1 - e^{-x} . \tag{2.45}$$

We then introduce the quantity, the maximum value of the normalised power,

$$Z(N) \triangleq \max\{X_n\}_{n=1}^{N} . \tag{2.46}$$

where $\{X_n\}_{n=1}^{N}$ is the set of X received from measurements performed at N independent stirrer positions. Every X_n is in itself a random variable with the distribution functions of (2.44) and (2.45). The cumulative distribution function of Z is,

[13] It does also exist a form of Radiated Susceptibility Test (RST) where the stirrer(s) is (are) moved continuously. That type of RST, often called mode stirring, is not explicitly addressed in this article.

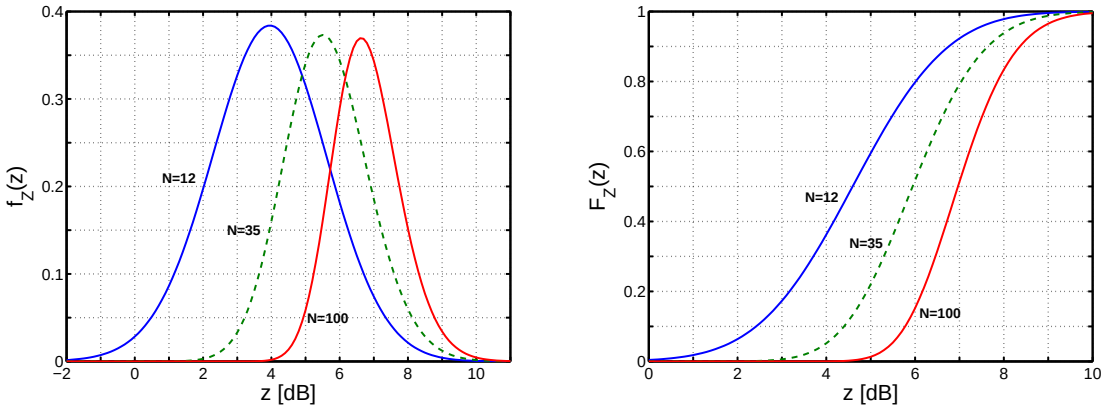

Figure 2.1: The probability density function and the cumulative density function, respectively, of the random variable *the maximum value of the normalised power* (Z), see (2.46). The functions are plotted for 12, 35 and 100 numbers of independent samples.

$$F_Z(z) \;=\; \mathbb{P}(Z \leq z) = \mathbb{P}(\text{All } X_n \leq z) = (1 - e^{-z})^N \;, \tag{2.47}$$

and the probability distribution function,

$$f_Z(z) \equiv \frac{\mathrm{d}F_Z(z)}{\mathrm{d}z} = N(1 - e^{-z})^{N-1} e^{-z} \;. \tag{2.48}$$

Equation (2.48) is a very fascinating result, *the distribution of the maximum power received in our EUT compared to the expected value of the (average) received power is only dependent on the number of (independent) stirrer positions (N) in use.* It does not depend on the EUT, and it does not further depend on the RC as long as (2.15) is fulfilled. The expected value of the (average) received power in the EUT is given in (2.42). It depends on the energy density in the RC through the constant C, the radiation efficiency (η) and the impedance mismatch factor (q) seen by the critical component in the EUT. That is all!

The distribution functions in (2.47) and (2.48) are plotted in Fig. 2.1 for 12, 35 and 100, respectively, numbers of independent stirrer positions.[14] For later purposes, we calculate the expectation value of the maximum value of the normalised power,

[14] At a first glance it might look strange that there is a, though small, probability that the maximum value is smaller than the expected value. However, it is not at all strange, it is only a good example showing the difference between expected value and average value. For a set of independent samples of a random variable, the average value will converge to the expected value when the number of elements in the set becomes very large. However, for a small number of elements in the set there is a finite probability that all values, including the maximum value, is smaller than the expected value.

$$\begin{aligned}\mathbb{E}\{Z\} &= \int_0^\infty z f_Z(z)\mathrm{d}z = \int_0^\infty zN(1-e^{-z})^{N-1}e^{-z}\mathrm{d}z = \left\{y = e^{-z}\right\} \\ &= N\int_0^1 \ln\left(\frac{1}{y}\right)(1-y)^{N-1}\,\mathrm{d}y\ . \end{aligned} \tag{2.49}$$

The integral in (2.49) can be rewritten as a sum,

$$\mathbb{E}\{Z\} = -N\sum_{n=0}^{N-1}\binom{N-1}{n}\int_0^1 \ln y(-y)^n\mathrm{d}y = N\sum_{n=0}^{N-1}\binom{N-1}{n}\frac{(-1)^n}{(n+1)^2}\ . \tag{2.50}$$

The expression in (2.50) is a finite form for the expectation value, but unfortunately the sum is not well behaved for large N, and it is then more beneficial to use the integral in (2.49).

2.3.2 T-distribution

The maximum value statistics of the normalised power, (2.47) and (2.48), are important. However, it is hard to test it experimentally when only a few independent stirrer positions are used. The reason being that we do not know the exact value of the expected value of the power (the denominator in (2.43)). We have to approximate it with the average value, and the average value is also a random variable. To analyse this, we start by defining the average normalised power,

$$Q(N) \triangleq \frac{1}{N}\sum_{m=1}^{N} X_m\ , \tag{2.51}$$

where X_m is the normalised power received for stirrer position m. All X_m are all samples of the same random variable X, (2.43), and do hence follow the same distribution, (2.44) and (2.45). The probability distribution function of Q is [17, p. 87 and 93],

$$f_Q(q) = \frac{N^N}{(N-1)!}q^{N-1}e^{-Nq}\ . \tag{2.52}$$

For large N, (2.52) can be approximated with help of Stirling's formula[15] as,

$$f_Q(q) \approx \sqrt{\frac{N}{2\pi}}q^{N-1}e^{-N(q-1)}, \quad N > 10\ . \tag{2.53}$$

[15] Stirling's formula says that for large N ($N > 10$), $N! \sim \sqrt{2\pi N}N^N e^{-N}$ [19, 16.16].

We now introduce the maximum to average random variable,

$$T(N) \triangleq \frac{Z(N)}{Q(N)} \ , \tag{2.54}$$

which we, compared to the random variable Z, more easily can do a statistical analysis of.[16] Before calculating the distribution functions of T, we prescribe that the two random variables Z and Q are independent. The cumulative distribution function of T can be calculated as [17, p. 96],

$$\begin{aligned} F_T(t) &= \int_0^\infty F_Z(qt) f_Q(q) \mathrm{d}q = \int_0^\infty (1-e^{-qt})^N \frac{N^N}{(N-1)!} q^{N-1} e^{-Nq} \mathrm{d}q = \left\{ y = e^{-Nq} \right\} \\ &= \frac{1}{(N-1)!} \int_0^1 \left[\ln\left(\frac{1}{y}\right) \right]^{N-1} \left[1 - y^{\frac{t}{N}} \right]^N \mathrm{d}y \ . \end{aligned} \tag{2.55}$$

The integral in (2.55) can be rewritten as a finite sum,

$$\begin{aligned} F_T(t) &= \frac{1}{(N-1)!} \sum_{n=0}^{N} \binom{N}{n} (-1)^n \int_0^1 \left[\ln\left(\frac{1}{y}\right) \right]^{N-1} y^{\frac{tn}{N}} \mathrm{d}y \\ &= \sum_{n=0}^{N} \binom{N}{n} (-1)^n \left(\frac{1}{1+\frac{n}{N}t} \right)^N . \end{aligned} \tag{2.56}$$

The expression in (2.56) is a finite form for the cumulative distribution function, but the sum is not well behaved and is difficult to numerically calculate for large N and small t. Unfortunately, the integral in (2.55) is not well behaved either. Luckily enough, the sum (2.56) is only badly behaved at so small values of t where the distribution function is so close to 0, that we simply can approximate as being exactly 0.

The probability density function is easily calculated outgoing from (2.55) and (2.56),

$$\begin{aligned} f_T(t) &\equiv \frac{\mathrm{d}F_T(t)}{\mathrm{d}t} = \frac{1}{(N-1)!} \int_0^1 \left[\ln\left(\frac{1}{y}\right) \right]^{N} \left[1 - y^{\frac{t}{N}} \right]^{N-1} y^{\frac{t}{N}} \mathrm{d}y \\ &= \sum_{n=1}^{N} \binom{N}{n} (-1)^{n+1} n \left(\frac{1}{1+\frac{n}{N}t} \right)^{N+1} . \end{aligned} \tag{2.57}$$

[16] For large values of N, Q will have a narrow distribution around 1, and T will converge toward Z.

The comments done to the calculation of (2.56) are equally applicable to the calculation of (2.57).

There is one important note to be emphasised; to be able to derive the distribution functions $F_T(t)$ and $f_T(t)$ as we did above, the two random variables Z and Q have to be independent [17, p. 96]. However, as we will see in section 4.2, that is fulfilled for the interesting case when we perform a Radiated Susceptibility Test in the Reverberation Chamber.

2.3.3 A-distribution

In some situations, typically a measurement situation with the purpose of characterising the RC, the two random variables Z and Q are calculated from the same ensemble. For that situation we define the random variable,[17]

$$A(N) \triangleq \left.\frac{Z(N)}{Q(N)}\right|_{\substack{\text{same}\\ \text{ensemble}}} . \tag{2.58}$$

The two random variables, T and A, are almost identical, but the difference is to be stressed once again. For, T the maximum and mean values are calculated from two independent ensembles. For A, the maximum and mean values are calculated from the same ensemble, and consequently the numerator and denominator in (2.58) are dependent on each other. It is much harder to find the distribution functions for A than for T. A literature study shows that almost all theory assume independent random variables. However, we will here derive the distribution functions for A. We start by rewriting (2.58),

$$A(N) = \frac{Z(N)}{\frac{1}{N}\sum_{n=1}^{N} X_n} = \frac{N}{1+\sum_{n=1}^{N-1}\frac{X_n}{Z(N)}} = \frac{N}{1+\sum_{n=1}^{N-1} C_n(N)} = \frac{N}{1+B(N)} , \tag{2.59}$$

where we without loss off generality rearrange the normalised power values so that the N:th one is the largest,

$$Z(N) \equiv X_N , \tag{2.60}$$

In (2.59) we also introduce the two random variables,[18]

$$C(N) \triangleq \frac{X}{Z(N)} , \tag{2.61}$$

$$B(N) \triangleq \sum_{n=1}^{N-1} C_n(N) , \tag{2.62}$$

[17] The random variable A is not to be confused with the index A introduced in section 2.1.

[18] The random variable B is not to be confused with the index B introduced in section 2.1.

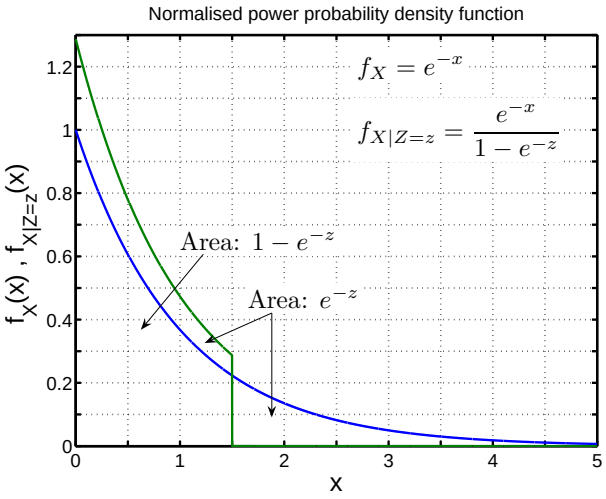

Figure 2.2: The blue dashed curve shows the probability density function for X, and the green dashed curve shows the probability density function for X given that is maximum value is not larger than z. When we include the condition that the maximum value of X is not larger than z, the value of the probability density function has to be increased for $0 < x < z$ so that the total probability remains 1.

The $N-1$ random variables C_n are dependent on each other through the common denominator Z, but let us, just for a while, assume that Z has a fixed value z. Then the C_n are among themselves independent because we do already from the beginning assume that the $N-1$ random variables X_n are independent. The pdf for C given that $Z = z$, is [17, p. 87],

$$f_{C|Z=z}(c) = z f_{C|Z=z}(zc) = \begin{cases} 0, & c < 0 \\ \frac{ze^{-zc}}{1-e^{-z}}, & 0 < c < 1 \\ 0, & c > 1 \end{cases} , \tag{2.63}$$

where we in the last step have renormalized the pdf in (2.44) to our case where $X \leq z$. How this renormalizing is done can be seen in Fig. 2.2. The total probability is always exactly 1, which in Fig. 2.2 is manifested by that the area under the probability density function is 1. When we include the condition that $X \leq z$, the probability of the remaining possible values of X are increased so that the total probability remains one. The relative probability among the remaining possible values of X is not to be changed. In (2.63) we have also explicitly included that $C|Z = z$ equals 0 outside the interval $[0, 1]$. Thereby we have defined $C|Z = z$ on the whole real axis.

The pdf for B given that $Z = z$, is [17, p. 92],

$$\begin{aligned} f_{B|Z=z}(b) &= f_{C_1|Z=z}(c) * f_{C_2|Z=z}(c) * \ldots * f_{C_{N-1}|Z=z}(c) \\ &= \mathfrak{F}^{-1}\left\{\mathfrak{F}\left\{f_{B|Z=z}\right\}\right\} = \mathfrak{F}^{-1}\left\{\left(\mathfrak{F}\left\{f_{C|Z=z}\right\}\right)^{N-1}\right\} . \end{aligned} \tag{2.64}$$

The use of the inverse Fourier transform ($\mathfrak{F}^{-1}$) and the Fourier transform ($\mathfrak{F}$) in (2.64) is a classical technique to analytically calculate convolutions. The Fourier transform of (2.63) is after some analysis found to be,

$$\mathfrak{F}\left\{f_{C|Z=z}\right\}(\omega) = \frac{z}{1-e^{-z}}\frac{1-e^{-(z+i\omega)}}{z+i\omega}, \tag{2.65}$$

and by use of the binominal formula [19, p. 3],

$$\left(\mathfrak{F}\left\{f_{C|Z=z}\right\}\right)^{N-1}(\omega) = \left(\frac{z}{1-e^{-z}}\right)^{N-1}\sum_{n=0}^{N-1}\binom{N-1}{n}(-1)^n\frac{e^{-nz}e^{-in\omega}}{(z+i\omega)^{N-1}}\ , \tag{2.66}$$

By performing the inverse Fourier transform in (2.64) we get,

$$f_{B|Z=z}(b) = \left(\frac{z}{1-e^{-z}}\right)^{N-1}e^{-zb}\sum_{n=0}^{N-1}\binom{N-1}{n}(-1)^n\frac{(b-n)^{N-2}}{(N-2)!}H(b-n)\ , \tag{2.67}$$

where we have introduced the Heaviside step function,

$$H(y) = \begin{cases} 0, & y<0 \\ 1, & y>0 \end{cases}\ . \tag{2.68}$$

By using the law of total probability [17, p. 34], we can calculate the joint pdf with help of (2.48) and (2.67),

$$\begin{aligned} f_{B,Z}(b,z) &= f_{B|Z=z}(b)f_Z(z) \\ &= N\sum_{n=0}^{N-1}\binom{N-1}{n}(-1)^n\frac{(b-n)^{N-2}}{(N-2)!}H(b-n)z^{N-1}e^{-z(b+1)}\ . \end{aligned} \tag{2.69}$$

We thereby have released the condition that $Z=z$, and we can calculate the pdf of B as the marginal pdf of (2.64),

$$\begin{aligned} f_B(b) &= \int_0^\infty f_{B,Z}(b,z)\mathrm{d}z \\ &= N\sum_{n=0}^{N-1}\binom{N-1}{n}(-1)^n\frac{(b-n)^{N-2}}{(N-2)!}H(b-n)\int_0^\infty z^{N-1}e^{-z(b+1)}\mathrm{d}z \\ &= \frac{N(N-1)}{(b+1)^N}\sum_{n=0}^{N-1}\binom{N-1}{n}(-1)^n(b-n)^{N-2}H(b-n)\ . \end{aligned} \tag{2.70}$$

We are now close to the goal of calculating the pdf and the cdf of A. The cdf of A can with help of (2.59) be written as,

$$F_A(a) \equiv \mathbb{P}(A \leq a) = \mathbb{P}\left(\frac{N}{1+B} \leq a\right) = \mathbb{P}(B \geq \frac{N}{a} - 1) = 1 - F_B\left(\frac{N}{a} - 1\right) \ , \quad (2.71)$$

and the pdf of A is with help of (2.70) found to be,

$$\begin{aligned} f_A(a) &\equiv \frac{\mathrm{d}F_A(a)}{\mathrm{d}a} = \frac{N}{a^2} f_B\left(\frac{N}{a} - 1\right) \\ &= \frac{(N-1)a^{N-2}}{N^{N-2}} \sum_{n=0}^{N-1} \binom{N-1}{n} (-1)^n \left(\frac{N}{a} - 1 - n\right)^{N-2} H\left(\frac{N}{a} - 1 - n\right) \\ &= (N-1) \sum_{n=0}^{N-1} \binom{N-1}{n} (-1)^n \left(1 - \frac{n+1}{N} a\right)^{N-2} \left[1 - H\left(a - \frac{N}{n+1}\right)\right] \\ &= (N-1) \sum_{n=0}^{\lfloor \frac{N}{a} - 1 \rfloor} \binom{N-1}{n} (-1)^n \left(1 - \frac{n+1}{N} a\right)^{N-2} \ , \end{aligned} \quad (2.72)$$

where the sign $\lfloor \ \rfloor$ denotes the integer part. The cdf of A is,[19]

[19]The random variable A is enclosed to the interval $[1, N]$. Hence the lower integration limit should be 1. However, as we in 2.63 have defined the pdf on the whole real axis, all the derived pdf are also valid on the whole real axis. Every value of a outside the interval $[1, N]$ plugged into 2.72 will automatically give 0 as result. That justifies the expansion of the integration interval down to 0. The reason for doing such an expansion is that it substantially simplifies the calculations. The one interested can put in 1 as the lower integration limit and go through some rather tedious calculations and finally end up with the same answer as in 2.73.

$$
\begin{aligned}
F_A(a) &\equiv \int_1^a f_A(a)\mathrm{d}a = \int_0^a f_A(a)\mathrm{d}a \\
&= (N-1)\sum_{n=0}^{N-1}\binom{N-1}{n}(-1)^{n+1}\int_0^{\min\left\{a,\frac{N}{n+1}\right\}}\left(1-\frac{n+1}{N}x\right)^{N-2}\mathrm{d}x \\
&= \sum_{n=0}^{N-1}\binom{N}{n+1}(-1)^{n+1}\left[\left(1-\frac{n+1}{N}x\right)^{N-1}\right]_0^{\min\left\{a,\frac{N}{n+1}\right\}} \\
&= \sum_{m=0}^{N}\binom{N}{m}(-1)^m\left[\left(1-\frac{m}{N}\min\left\{a,\frac{N}{m}\right\}\right)^{N-1}-1\right] \\
&= \sum_{m=0}^{\left\lfloor\frac{N}{a}\right\rfloor}\binom{N}{m}(-1)^m\left[\left(1-\frac{m}{N}a\right)^{N-1}-1\right]-\sum_{m=\left\lfloor\frac{N}{a}\right\rfloor+1}^{N}\binom{N}{m}(-1)^m \\
&= \sum_{m=0}^{\left\lfloor\frac{N}{a}\right\rfloor}\binom{N}{m}(-1)^m\left(1-\frac{m}{N}a\right)^{N-1}\quad . \qquad (2.73)
\end{aligned}
$$

The last two rows of calculations does somewhat simplify the expression, but more important, it gives an expression which is more well behaved for large N. For very large[20] N even the last expression is mathematically badly behaved, but only at the small values of a where we without any significant error can approximate $F_A(a)$ as being exactly 0.

The distribution functions for A are plotted in Fig. 2.3 for 12, 35 and 100, respectively, numbers of independent stirrer positions.

[20] At which N problems with the accuracy in the summation occur depends on the software (and the computer) in use. When using PC-MatLab, significant inaccuracies occurs when $N > 100$.

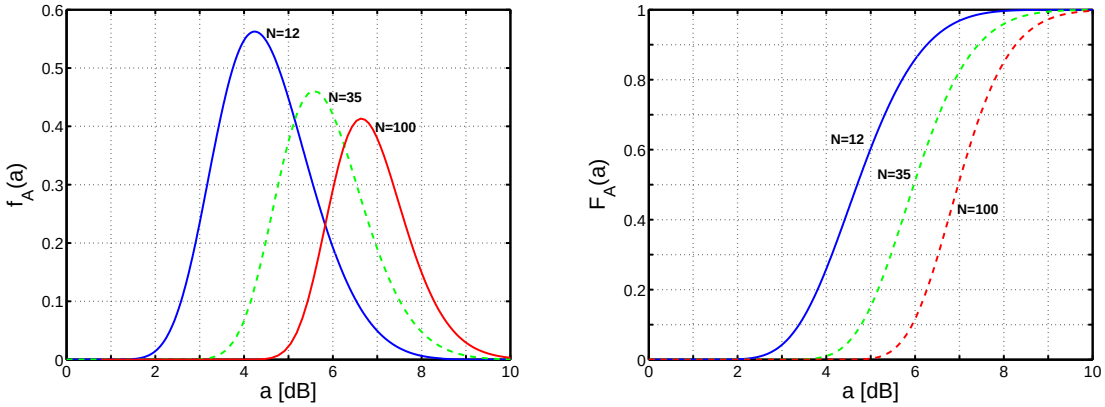

Figure 2.3: The probability density function and the cumulative density function, respectively, of the random variable A, see (2.58). The functions are plotted for 12, 35 and 100 numbers of independent samples.

Chapter 3

Experiments

3.1 Antennas as Equipment Under Test

To test the validity of the theory developed in chapter 2, we have performed measurements. The measurements were performed in our large Reverberation Chamber, with dimensions: 5.10m $\times$ 2.46m $\times$ 2.93m. The Lowest Useable Frequency (LUF) of the chamber depends on the exact definition of LUF and the type and numbers of stirrer in use. Anyhow in our measurements it is completely appropriate to use it above 1 GHz. All our measurements values are uncorrelated and we assume that it implies that the values also are independent [9].

First we used four different antennas, see Fig. 3.1, as Equipment Under Test (EUT). We transmitted electromagnetic power into our Reverberation Chamber (RC), and in four consecutive experiments we measured the power received in our four different antennas. In every experiment we measured the power for 200 different independent stirrer positions. For every measurement we calculated a sample of the random variable T. By also performing every measurements for 801 different frequencies equidistantly placed in the interval $8.2 - 12.4$ GHz, we could do a statistical analysis of the random variable T.[1]

The last paragraph in section 2.3.2 is again to be emphasised. In calculating the samples of T, the numerator and the denominator has to be independent. That can be done by measuring the maximum value and the average value with two different antennas, or by calculating the maximum value and the average value for two different frequencies. However, here we do it by simply calculating the maximum value using one half of the measurement values from the 200 independent stirrer positions, and the average value by using the other half. The reason is, that the radiation efficiency (η) and the impedance mismatch factor (q) do generally vary from antenna to antenna, and is also frequency dependent, and in the general case we have to compensate for that, but if we use the same antenna and the same frequency, the two factors will be identical in the numerator and the denominator in the calculations of the samples of

[1] To be able to perform a statistical analysis, it is important that the 801 samples are independent.

Figure 3.1: To test our theory we performed four experiments with these four antennas as Equipment Under Test.

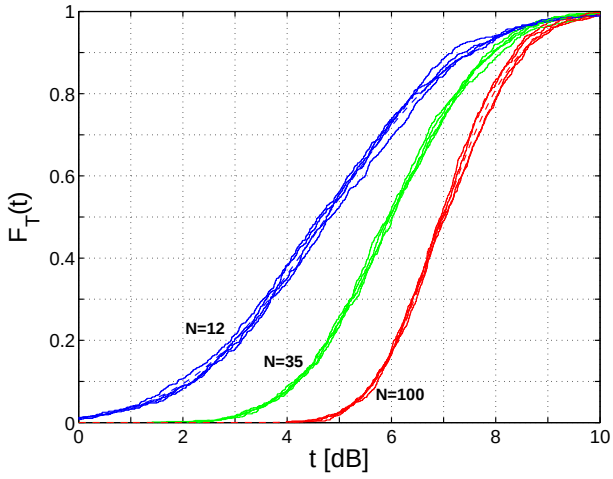

Figure 3.2: The cumulative distribution function for the random variable T is plotted with dashed lines for 12, 35 and 100 numbers of independent samples. The results of measurements on the four different antennas in Fig. 3.1 is plotted with solid lines. The difference in result between the four different antennas is small, and the agreement with theory is so good that the theoretical dashed lines are very difficult to observe.

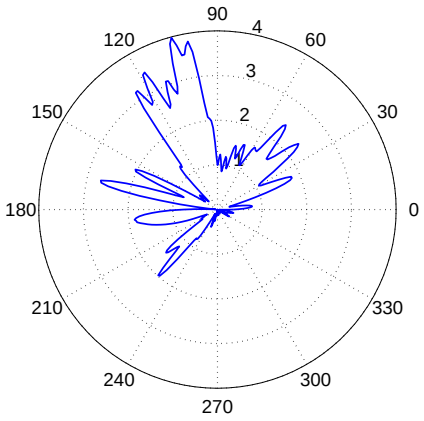

Figure 3.3: One example of how the received power by a pin antenna mounted inside a well shielded test object, see Fig. 3.4, varies with irradiation direction. The test object has been irradiated from 360 equidistant placed directions within one plane. The incident polarisation has been kept constant, the frequency is 3.0 GHz, and the received power has been normalised so that the average value is 1.

T, and will hence cancel each other. The price we have to pay is that we can only calculate samples of T for half as many independent stirrer positions as we measured.

In Fig. 3.2, the measurements of the random variable T are shown for 12, 35 and 100 independent samples. Each set of curves includes four measurement curves from the four different antennas, and somewhere in the middle the theoretical curve, calculated with (2.56).

3.2 Real Test Objects as Equipment Under Test

We were surprised by the good accuracy between theory and measurements in Fig. 3.2. The four antennas have different directivity patterns as well as different receiving polarisation patterns, and, as we discussed in the introduction, should not that affect the outcome of the experiments? We then argued that the directivity and receiving polarisation of constructed antennas does after all vary rather slowly with direction, and in chapter 2 we stated that the solid angle spectrum (of the electric field) in two different directions are completely uncorrelated. Perhaps, when we change the direction a little, the solid angle spectrum will go through all possible values, but the directivity and receiving polarisation of our antennas remain almost constant. Hence, every directivity and receiving polarisation of our antennas should see the same solid angle spectrum, and as a consequence thereof, we can for every antenna use the average directivity, which is 1 and the average polarisation efficiency, which is $\frac{1}{2}$.

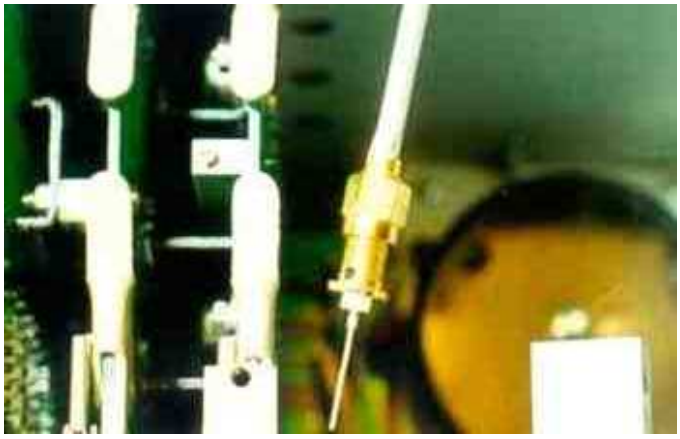

Figure 3.4: The power received by a pin antenna mounted inside the test object represents the typical power received by a wire inside the test object.

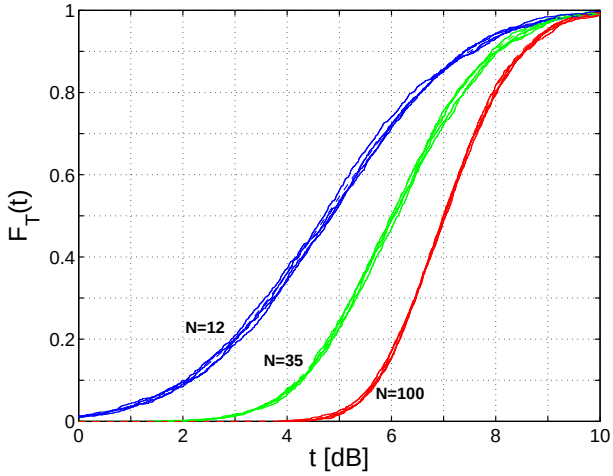

Figure 3.5: The cumulative distribution function for the random variable T is plotted with dashed lines for 12, 35 and 100 numbers of independent samples. The results of measurements on the four different real test objects are plotted with solid lines. Like in Fig. 3.2, the difference in result between the four different objects is small, and the agreement with theory is so good that the theoretical dashed lines are very difficult to observe.

However, every model has its limitation in validity. Well shielded test objects, has a directivity and receiving polarisation pattern which varies rapidly with irradiation direction, see Fig. 3.3. We therefore decided to use four different types of well shielded objects as Equipment Under Test, one explicitly constructed to be well shielded. The objects are all real objects filled with different forms of electronics. They have different forms and sizes, but the volumes are in the order of a tenth of cubic decimetre to tens of a cubic decimetre. We mounted a pin antenna inside the test object to be able to receive electromagnetic power, see Fig. 3.4. The pin antenna represents a typical short wire inside the test object. We thought that by testing these objects with rapidly varying directivity and receiving polarisation patterns, we would overstep the validity of (2.15) which is the foundation for the development of all theory in this article.

We performed the same measurements as in section 3.1, but now with our four real test objects as Equipment Under Test instead of the four antennas. This time we used 1334 different frequencies in the interval $1 - 18$ GHz. The result can be seen in Fig. 3.5. The agreement between theory and measurements is just as good as in Fig. 3.2. We conclude that the theory which we have developed is valid for the practical cases which we are interested in, and the doubts, which we have brought up, we do not have to consider any longer.

3.3 Experiments on the A-distribution

We also want to experimentally verify the derivation of the A-distribution (section 2.3.3). That we do by using the same measurement data as in section 3.1, but with the important exception that we here calculate the maximum and average values from the same set of measurement data. The result is shown in Fig. 3.6. The measurements of the random variable A are plotted for 12, 35 and 100 numbers of independent samples. Each bunch of curves includes the measurements results from the four different antennas in Fig. 3.1 (4 solid lines) as well as the theoretical expression according to (2.73) plotted with a dashed line. Again, the agreement between theory and experiments is very good.

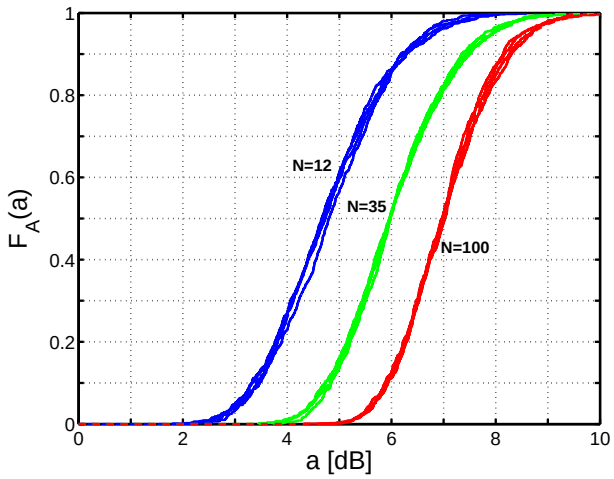

Figure 3.6: The cumulative distribution function for the random variable A is plotted with dashed lines for 12, 35 and 100 numbers of independent samples. The results of measurements on the four different antennas in Fig. 3.1 are plotted with solid lines. Like in Fig. 3.2, the difference in result between the four different antennas is small, and the agreement with theory is so good that the theoretical dashed lines are very difficult to observe.

Chapter 4

Practical Advice on using the Reverberation Chamber for Radiated Susceptibility Testing

Fig. 4.1 shows an example of how a Radiated Susceptibility Test (RST) may be performed. A transmitting antenna transmits electromagnetic energy into the chamber, and part of that electromagnetic energy is absorbed by the critical component in the Equipment Under Test (EUT) as well as by the reference antenna. The test procedure is performed for N independent stirrer positions. The power absorbed in the critical component, as well as the power absorbed in the reference antenna, differs from stirrer position to stirrer position, but the expected value can (in theory) be calculated with help of (2.42). The expected value of the power being absorbed in the reference antenna is in practical cases much larger than the expected value for the power being absorbed in the critical component. The reason being that the reference antenna is a manufactured optimised antenna with impedance mismatch factor (q) as well as radiation efficiency (η) close to 100%. The EUT, with the critical component as load, is not an optimised antenna. In opposite it is often optimised to be an as bad antenna as possible, and low values of the impedance mismatch factor and the radiation efficiency does actually constitute that the critical component is well shielded [20].

In performing an RST we do not focus on measuring the power being absorbed in the critical component, but what is the stress we put onto our EUT. A good measure of that stress, is the power which would have been absorbed in the critical component of the EUT if the impedance mismatch factor and the radiation efficiency both had been equal to 1. Exactly that power we measure in our reference antenna,[1] if we assume that the electromagnetic environment seen by the reference antenna is the same as the one seen by the EUT. The measurement is preferably performed like in Fig. 4.1 with both the EUT and the reference antenna in the RC at the same time,

[1] We assume that both the impedance mismatch factor and the radiation efficiency of the reference antenna equal 1. If not, we can easily compensate for that.

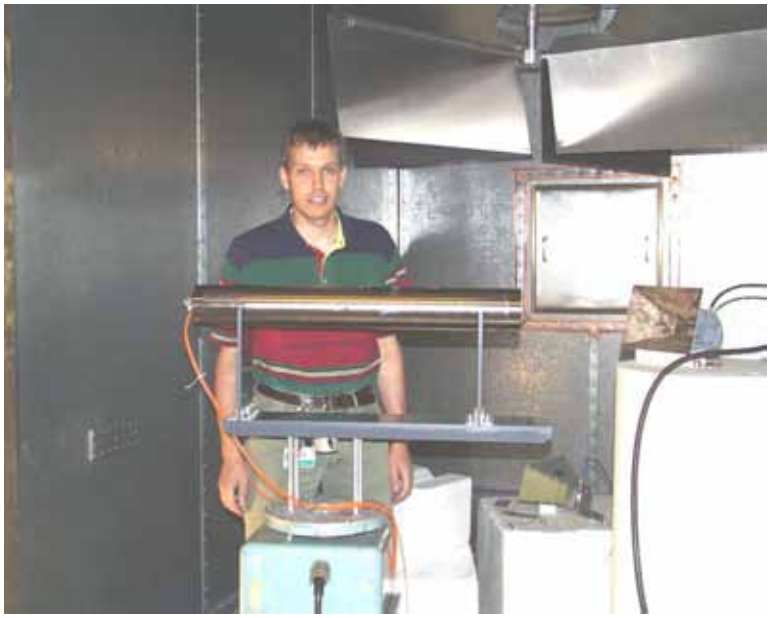

Figure 4.1: A typical Radiated Susceptibility Test (RST). One of the antennas transmits electromagnetic energy into the Reverberation Chamber (RC). The other antenna measures the stress we put onto the Equipment Under Test (EUT). (In this figure the generic missile GENEC is the EUT. The author is to be taken out of the chamber before the test is performed.)

because then the reference antenna as well as the EUT see the same lowering of the Q-value caused by themselves.

4.1 Using Maximum Values

In the paragraph above we benefited from that the power stressed onto the EUT was the same as the power "stressed" onto (or differently stated, measured by) the reference antenna. That is true for the expected value, see (2.42), and hence a good approximation for the average over many independent stirrer positions. However, in an RST we are most often not interested in the average power we stress onto the EUT, but on the maximum power we stress onto the EUT. The maximum power is caused for one of the stirrer positions, and the maximum power stressed onto the EUT will differ from the maximum power "stressed" onto the reference antenna. That issue is in [21] and [22] addressed by assuming that, if we stress the EUT and the reference antenna at many (200 in [21] and [22]) independent stirrer positions, the maximum power stressed onto the EUT will be approximately the same as the maximum power "stressed" onto the reference antenna, though the maximum power is not generally reached for the same stirrer position. That assumption is however not completely true and we will now further examine the issue.

Let us introduce two random variables U and V, where U is the maximum power

stressed onto the EUT and V is the maximum power "stressed" onto the reference antenna. The maximum is taken over N independent stirrer positions. We then form the quotient,

$$W(N) \triangleq \frac{U(N)}{V(N)} = \frac{\frac{U(N)}{\mathbb{E}\{P\}}}{\frac{V(N)}{\mathbb{E}\{P\}}} \ . \tag{4.1}$$

The new random variable W is very interesting because it tells us what the power stressed onto our EUT is relative to the power measured in (or differently stated, stressed onto) the reference antenna. After the last equal sign in (4.1) we have divided both U and V with the expected value of the power stressed onto the EUT as well as the reference antenna.[2] Thereby we have two random variables, one in the numerator ($\frac{U}{\mathbb{E}\{P\}}$) and one in the denominator($\frac{V}{\mathbb{E}\{P\}}$), which are mutual independent and both have the same distribution functions as the random variable Z in (2.46).[3] As a consequence thereof we can calculate the cumulative distribution function of the random variable W as [17, p. 96],

$$\begin{aligned} F_W(w) &= \int_0^\infty F_Z(zw) f_Z(z) \mathrm{d}z = \int_0^\infty (1-e^{-zw})^N N(1-e^{-z})^{N-1} e^{-z} \mathrm{d}z = \left\{y = e^{-z}\right\} \\ &= N \int_0^1 (1-y^w)^N (1-y)^{N-1} \mathrm{d}y \ . \end{aligned} \tag{4.2}$$

The integral in (4.2) can be rewritten as a finite double sum,

$$\begin{aligned} F_W(w) &= N \int_0^1 \sum_{m=0}^{N} \binom{N}{m} (-1)^m y^{wm} \sum_{n=0}^{N-1} \binom{N-1}{n} (-1)^n y^n \mathrm{d}y \\ &= N \sum_{m=0}^{N} \sum_{n=0}^{N-1} \binom{N}{m} \binom{N-1}{n} \frac{(-1)^{m+n}}{mw+n+1} \ . \end{aligned} \tag{4.3}$$

The expression in (4.3) is a finite form for the cumulative distribution function, but the sums are not well behaved and are difficult to numerically calculate for large

[2] As described above the expected value of the stressed power onto the EUT equals the expected value for the power stressed onto the reference antenna, so we do not have to worry about which one to use.

[3] In section 2.3 we focus on the power received by an object, here we focus on the power being stressed onto that object. The difference is all the time the product of the impedance mismatch factor (q) and the radiation efficiency (η). However by defining random variables where we divide by expectation values this product will cancel, and hence we will get the same distribution functions.

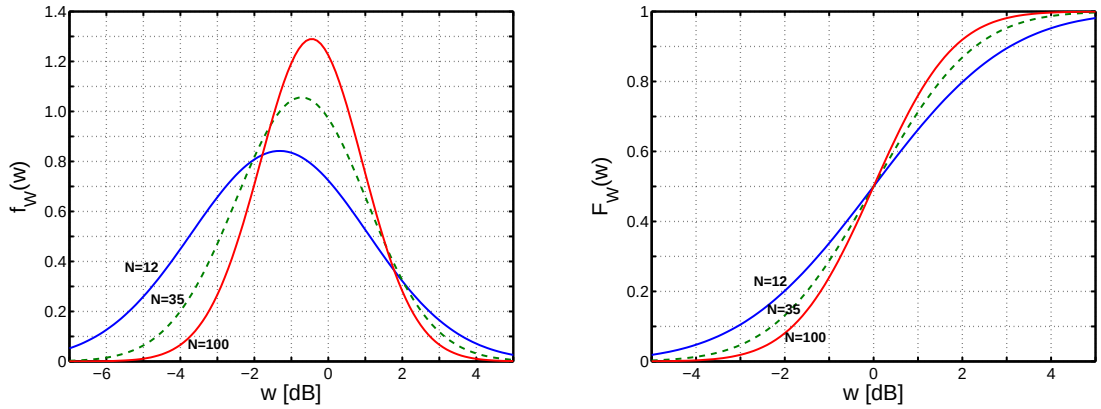

Figure 4.2: The probability density function and the cumulative density function, respectively, of the random variable W, see (4.1). The functions are plotted for 12, 35 and 100 numbers of independent samples.

N. It is actually more beneficial to numerically calculate the cumulative distribution function with help of the integral in (4.2). The probability density function is easily calculated outgoing from (4.2) and (4.3),

$$\begin{aligned} f_W(w) &\equiv \frac{\mathrm{d}F_W(w)}{\mathrm{d}w} = N^2 \int_0^1 \ln\left(\frac{1}{y}\right) y^w \left[(1-y^w)(1-y)\right]^{N-1} \mathrm{d}y \\ &= N \sum_{m=0}^{N} \sum_{n=0}^{N-1} \binom{N}{m} \binom{N-1}{n} \frac{(-1)^{m+n+1} m}{(mw+n+1)^2} \ . \end{aligned} \tag{4.4}$$

Again, the sums are not well behaved for large N, and it is more beneficial to use the integral.[4] In Fig. 4.2, the distribution functions in (4.3) and (4.4), respectively, are plotted for 12, 35 and 100 numbers of independent samples.

We now know the distribution of W, and by solving the equation,

$$1 - \alpha = F_W(w_\alpha) \ , \tag{4.5}$$

for

$$w_\alpha = F_W^{-1}(1-\alpha) \ , \tag{4.6}$$

[4]The function $\ln(\frac{1}{y})$ has a pole at $y = 0$ and that may cause some numerical problems. However, the product $\ln(\frac{1}{y})y^w$ does not have a pole at $y = 0$, actually it has a zero at $y = 0$, and the product can with help of the l'Hôpital's rule be shown to equal $\frac{y^w}{w}$ at $y = 0$. By approximating $\ln(\frac{1}{y})y^w$ with $\frac{y^w}{w}$ at the lower end of the interval, the numerical difficulties disappear.

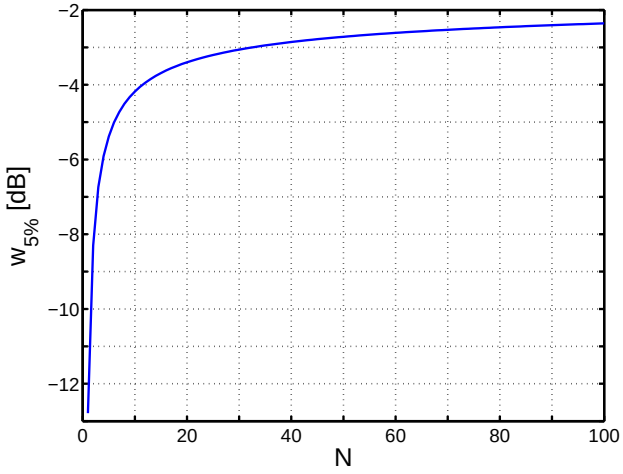

Figure 4.3: By multiplying the maximum power value measured in our reference antenna by the factor $w_{5\%}$, we get a power value which by 95% confidence is lower than the power stressed onto our EUT.

we can conclude that by $1-\alpha$ confidence, the power stressed onto the EUT is larger than w_α times the maximum power measured in our reference antenna. In Fig. 4.3 $w_{5\%}$ is plotted as function of the number of independent stirrer positions. We can (with a good eyesight) see in Fig. 4.3 that if we e.g. uses 12 independent stirrer positions, we have to subtract a security margin of 3.9 dB from the power measured in the reference antenna to get a power value which with 95 % confidence is smaller than the one stressed onto the EUT.

4.2 Using Average Values

We may actually do slightly better than the maximum value method proposed in section 4.1. By only using the maximum value from N independent stirrer positions, we do not use much of the information from the other $N-1$ independent stirrer positions. Let us instead use the average power measured in our reference antenna, where the average is taken over N independent stirrer positions. The random variable T, defined in (2.54), tells us how the maximum power stressed onto the EUT is distributed compared to the average power measured in the reference antenna. The probability density function (2.57) and the cumulative density function (2.55), respectively, are in Fig. 4.4 plotted for 12, 35 and 100 numbers of independent samples. In complete similarity to (4.5) we solve the equation,

$$1-\alpha = F_T(t_\alpha)\ , \tag{4.7}$$

for

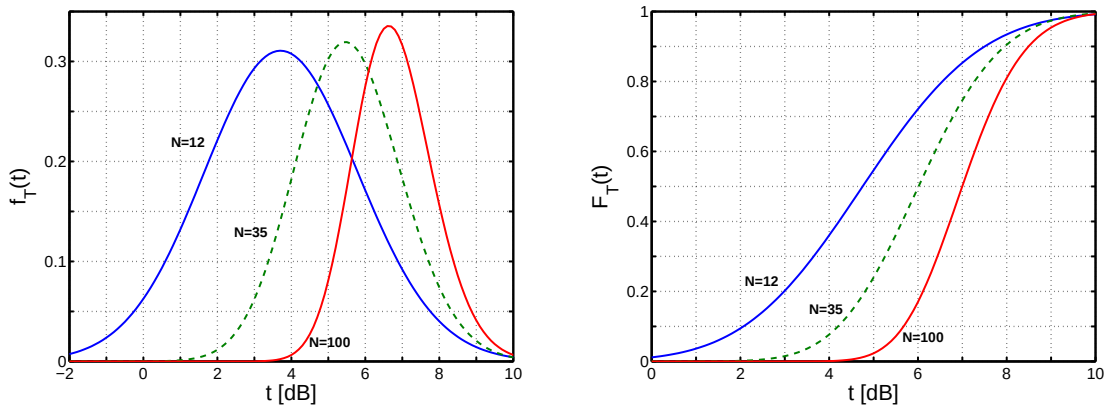

Figure 4.4: The probability density function and the cumulative density function, respectively, of the random variable T, see (2.54). The functions are plotted for 12, 35 and 100 numbers of independent samples.

$$t_\alpha = F_T^{-1}(1-\alpha) \ . \tag{4.8}$$

Then we can state that by $1-\alpha$ confidence, the power stressed onto the EUT is larger than t_α times the power measured in our reference antenna. In Fig. 4.5, $t_{5\%}$ is plotted as function of the number of independent stirrer positions. We can (with a good eyesight) see in Fig. 4.5 that if we e.g. uses 12 independent stirrer positions, we can add 1.3 dB to the average power measured in the reference antenna to get a power value which with 95 % confidence is smaller than the one stressed onto the EUT.

4.3 Comparing the Average Value Method to the Maximum Value Method

Independent of whether the maximum value method, proposed in section 4.1, or the average value method, proposed in section 4.2, is used, the true stress onto the EUT is, of course, the same. In both cases we also have to measure the power in the reference antenna for every stirrer position. The two methods are in that respect identical. However, they will not give the same answer to the question of to which power level we have tested our EUT. The test level is for the maximum value method,

$$Z_T = w_\alpha Z \ , \tag{4.9}$$

and for the average value method,

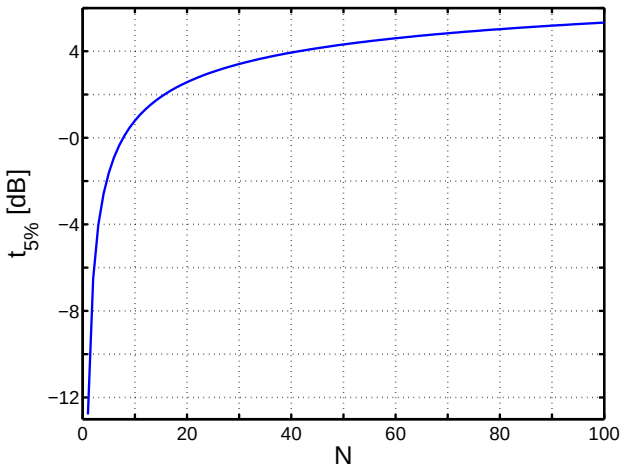

Figure 4.5: By multiplying the average power value measured in our reference antenna by the factor $t_{5\%}$, we get a power value which by 95% confidence is lower than the power stressed onto our EUT.

$$Q_T = t_\alpha Q \ . \tag{4.10}$$

The two test power levels are them selves random variables, with probability density functions [17, p. 87],

$$f_{Z_T}(z_T) = \frac{1}{w_\alpha} f_Z(\frac{z_T}{w_\alpha}) \ , \tag{4.11}$$

and,

$$f_{Q_T}(q_T) = \frac{1}{t_\alpha} f_Q(\frac{q_T}{t_\alpha}) \ , \tag{4.12}$$

respectively.

An easy way to compare the two test methods is to relate the expectation values of the test power level for the average value method to the test power level for the maximum value method,

$$G(N,\alpha) \triangleq \frac{\mathbb{E}\{Q_T\}}{\mathbb{E}\{Z_T\}} = \frac{t_\alpha \mathbb{E}\{Q\}}{w_\alpha \mathbb{E}\{Z\}} = \frac{t_\alpha(N)}{w_\alpha(N)\mathbb{E}\{Z(N)\}} \ . \tag{4.13}$$

In Fig. 4.6, G at the 95% confidence level ($\alpha = 5\%$) is plotted as function of the number of independent stirrer positions. Obviously, there is a small advantage in

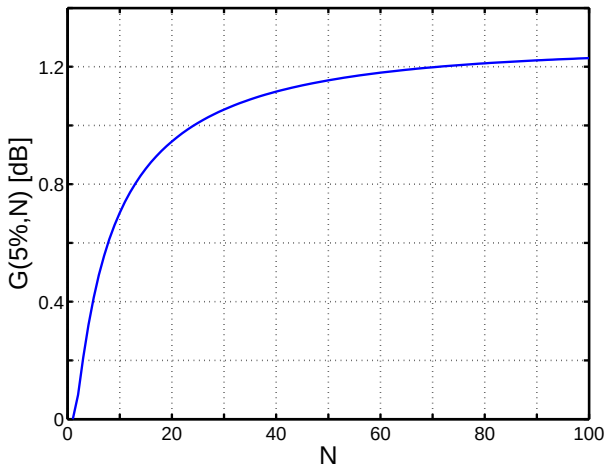

Figure 4.6: The figure shows the expected test power level when the average value method is used relative to the expected test power level when the maximum value method is used.

using the average value method. Fig. 4.7 shows another advantage with the average value method; we have there plotted the probability density functions, (4.11) and (4.12), for 12 independent stirrer positions and 95% confidence level. The probability density function for Q_T is less spread out than Z_T, and hence we will by using the average value method get less variation in the test power level from time to time. Still another advantage of using average values is that the influence of other random measurement errors will be substantially reduced. Consequently, we recommend using the average value method.

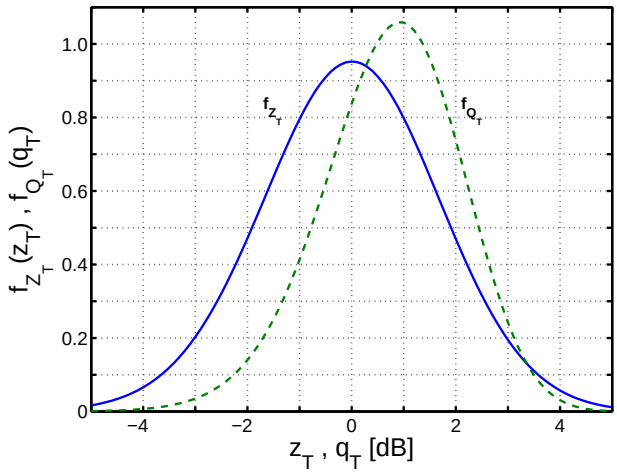

Figure 4.7: The probability density functions for the two test variables Z_T and Q_T.

Chapter 5

Summary

In assuming that the electromagnetic environment in the Reverberation Chamber (RC) is completely described by (2.15) we show that the power received in the Equipment Under Test (EUT) is neither affected by the directivity pattern or the receiving polarisation pattern of the EUT. Most physical descriptions are approximations, and we assume that for an EUT with a directivity pattern and/or receiving polarisation pattern which vary very rapidly as function of direction, it should be possible to reach the limit for the validity of (2.15). However, we have by testing real EUT's with rapidly varying directivity and receiving polarisation patterns not managed to reach the limit of the validity of (2.15). We therefore conclude that, when we perform a Radiated Susceptibility Testing in the Reverberation Chamber, we are within the validity of (2.15).

In performing a Radiated Susceptibility Test (RST), the power stressed onto the EUT is measured by a reference antenna in the RC. The power stressed onto the EUT does differ from the power measured by the antenna, but by taking the average measured power in the reference antenna and multiplying the result with the factor in (4.8), we get a test power level for the RST. The power stressed onto the EUT is with a prescribed confidence $(1 - \alpha)$ larger than the test power value.

Acknowledgement

The measurements presented in chapter 3 were performed by Olof Lundén, Leif Jansson and Jörgen Lorén. We thank Mats Bäckström for valuable expertise and being a good project leader. We thank prof. Gerhard Kristensson for being a good teacher and some fruitful discussions.

Appendix A

An Integral

In the calculations done in this article we have used the following integral [19, 15.90],

$$\int_0^1 (\ln y)^n y^m \mathrm{d}y = \frac{(-1)^n n!}{(m+1)^{n+1}}, \qquad \begin{matrix} m > -1 \\ n = 0, 1, 2, ... \end{matrix} \quad . \tag{A.1}$$

References

[1] J. G. Kostas and B. Boverie. Statistical model for a mode-stirred chamber. *IEEE Trans. Electromagn. Compat.*, 33:366–370, November 1991.

[2] D. A. Hill. Plane wave integral representation for fields in reverberation chambers. *IEEE Trans. Electromagn. Compat.*, 40:209–217, August 1998.

[3] D. A. Hill. Electromagnetic theory of reverberation chambers. NIST Technical Note 1506, National Institute of Standards and Technology (NIST), U.S. Dept. of Commerce, 325 Broadway, Boulder, CO 80303-3328, USA, December 1998.

[4] T. H. Lehman. A statistical theory of electromagnetic fields in complec cavities. Interaction Note 494, USAF Phillips Laboratory, Kirtland AFB, NM 87117-6008, USA, May 1993.

[5] M. Höijer, M. Bäckström and J. Lorén. Angular patterns in low level coupling measurements and in high level radiated susceptibility testing. In *Proc. International Zurich Symposium and Technical Exhibition on Electromagnetic Compatibility*, pages 347–352, Zürich, Switzerland, August 18–20, 2003.

[6] M. Höijer. Reduction of the uncertainty in radiated susceptibility testing by introduction of the compound polarisation efficiency. In *Proc. International Zurich Symposium and Technical Exhibition on Electromagnetic Compatibility*, pages 347–352, Zürich, Switzerland, February 13–18, 2005.

[7] M. Höijer. Comparison between high level radiated susceptibility tests and coupling measurements. Technical Report FOI-R--0562--SE, Swedish Defence Research Agency (FOI), SE-581 11 Linköping, Sweden, September 2002.

[8] J. Ladbury, G. Koepke, and D. Camell. Evaluation of the NASA Langley research center mode-stirred chamber facility. NIST Technical Note 1508, National Institute of Standards and Technology (NIST), U.S. Dept. of Commerce, 325 Broadway, Boulder, CO 80303-3328, USA, January 1999.

[9] N. Wellander, Olof Lundén and M. Bäckström. The maximum value distribution in a reveberation chamber. In *Proc. IEEE International Symposium on Electromagnetic Compatibility*, pages 751–756, Montréal, Canada, August 13–17, 2001.

[10] J. A. Stratton. *Electromagnetic Theory*, chapter VII. McGraw-Hill, New York, NY, 1941.

[11] G. Kristensson, prof., Electromagnetic Theory Group, Dept. of Electroscience, Lund University, Sweden, EU. private communication, 2005.

[12] M. Höijer, O. Lundén and M. Bäckström. Reverberation chamber: The quest for the distribution of the maximum stress onto the equipment under test. In *EMC Europe International Symposium on Electromagnetic Compatibility*, Barcelona, Catalonia, Spain, EU, September 4–8, 2006.

[13] G. R. Grimmett and D. R. Stirzaker. *Probability and Random Processes*. Oxford University Press, Oxford, UK, 1990. ISBN 0-19-853185-0.

[14] C. A. Balanis. *Antenna Theory : Analysis and Design*. John Wiley & Sons, New York, NY, 1997. ISBN 0-471-59268.

[15] W. L. Stutzman and G. A. Thiele. *Antenna Theory and Design*. John Wiley & Sons, New York, NY, 1981. ISBN 0-471-04458-X.

[16] IEEE Std 145-1983. IEEE Standard Definitions of Terms for Antennas. *IEEE Trans. Antennas Propagat.*, 31(6, Part II of 2 parts):5–29, November 1983.

[17] G. Blom. *Sannolikhetsteori och statistikteori med tillämpningar*. Studentlitteratur, Lund, Sweden, 1980. ISBN 91-44-03593-4.

[18] O. Lundén and M. Bäckström. Stirrer efficiency in FOA reverberation chambers. evaluation of correlation coefficients and chi-squared tests. In *Proc. IEEE International Symposium on Electromagnetic Compatibility*, pages 11–16, Washington, DC, USA, August 21–25, 2000.

[19] M. R. Spiegel. *Mathematical Handbook of Formulas and Tables*. McGraw-Hill, New York, NY, 1968.

[20] M. Höijer, V. Isovic and M. Bäckström. Electromagnetic transfer effectiveness of complex electronic equipment. Technical Report FOI-R--1395--SE, Swedish Defence Research Agency (FOI), SE-581 11 Linköping, Sweden, December 2004.

[21] M. Höijer and M. Bäckström. How we confused the comparison between high level radiated susceptibility measurements in the reverberation chamber and at the open area test site. In *IEEE Int. Symp. on EMC*, pages 1043–1046, Istanbul, Turkey, May 11–16, 2003.

[22] M. Höijer and M. Bäckström. A comparison of high level radiated susceptibility measurements in the reverberation chamber and at the open area test site. In *Proc. RadioVetenskap och Kommunikation 05*, pages 471–476, Linköping, Sweden, EU, June 14–16, 2005.